Observing Application

Date:	Feb 01, 2022
Proposal ID:	GBT/22B-242
Legacy ID:	QM488
PI:	Brian Mason
Type:	Regular
Category:	High Redshift and Source Surveys
Total time:	18.75

Measuring 3mm Source Contamination in the ACT Galaxy Cluster Sample

Abstract:

We propose 3mm GBT continuum imaging of 111 more galaxy clusters to our in progress survey of 300 clusters selected from the Atacama Cosmology Telescope (ACT) survey. We are using the tremendous point source survey speed of the GBT to more accurately characterize the thermal and non-thermal discrete sources-- mostly star forming galaxies or Active Galactic Nuclei (AGN), which can be cluster members, foreground sources, or background sources-- and their evolution with redshift. From the point of view of Sunyaev-Zeldovich Effect (SZE or SZ) cluster surveys, these sources represent a source of noise-- or worse, of bias-- which according to our existing MUSTANG-2 measurements may be more significant than generally appreciated. Our survey will yield the most precise characterization to date of the extent to which these sources contaminate current and next generation SZ cluster surveys. The statistical constraints from our survey will be broadly applicable to current and next generation SZE surveys such as ACT, SPT, Simons Observatory, and CMB S4. In conjunction with radio (NVSS, FIRST, VLASS), infra-red (WISE), and deep optical data, they will also advance our understanding of the underlying astrophysical populations in the millimeter wavelength regime, yielding important, new constraints on their evolution.

Authors:

Name	Institution	Email	Status
Mason, Brian	National Radio Astronomy Observatory	bmason@nrao.edu	
Dicker, Simon	Pennsylvania, University of	simon.dicker@gmail.com	
Hilton, Matt	KwaZulu-Natal, University of	hiltonm@ukzn.ac.za	
Bhandarkar, Tanay	Pennsylvania, University of	tanayb@sas.upenn.edu	Graduating: N/A Thesis: false
Orlowski-Scherer, John	Pennsylvania, University of	jorlo@sas.upenn.edu	Graduating: N/A Thesis: false
Mroczkowski, Tony	European Southern Observatory	tony.mroczkowski@eso.org	
Romero, Charles	Center for Astrophysics | Harvard & Smithsonian	ceromero@sas.upenn.edu	
Sievers, Jonathan	McGill University	jonathan.sievers@mcgill.ca	
Moravec, Emily	Green Bank Observatory	emoravec@nrao.edu	
Sarazin, Craig	Virginia, University of	sarazin@virginia.edu	
Gralla, Megan	Arizona, University of	mgralla@pha.jhu.edu	
Battaglia, Nicholas	Cornell University	nb572@cornell.edu	
Devlin, Mark	Pennsylvania, University of	devlin@physics.upenn.edu	
Perez Sarmiento, Karen	Pennsylvania, University of	kaper@sas.upenn.edu	Graduating: 2025 Thesis: false

Name	Institution	Email	Status
Haridas, Saianeesh	Pennsylvania, University of	haridas@sas.upenn.edu	Graduating: N/A Thesis: false
Di Mascolo, Luca	Trieste, UniversitÃ degli Studi di	luca.dimascolo@units.it	

Principal Investigator: Brian Mason
Contact: Brian Mason
Telephone: +1(434)987-3051
Email: bmason@nrao.edu

Related Proposals:

GBT21B_298

Joint:

Not a Joint Proposal.

Observing type(s):

Continuum

GBT Resources

Name	Group	Frontend & Backend	Setup
M2 stuff (Shared Risk)	M2 hardware	Mustang 2 Mustang 2	Number of Banks: 0

Sources

Name	Position		Velocity		Group
ACT-CLJ0200.3+0019	**Coordinate system**	Equatorial	**Convention**	Optical	fall
	Equinox	J2000			
	Right Ascension	02:00:20.953	**Ref. frame**	Barycentric	
		00:00:00			
	Declination	+00:19:30.0	**Velocity**	0.0	
		00:00:00			
	Calibrator	No			
ACT-CLJ0201.6-0211	**Coordinate system**	Equatorial	**Convention**	Optical	fall
	Equinox	J2000			
	Right Ascension	02:01:41.7135	**Ref. frame**	Barycentric	
		00:00:00			
	Declination	-2:11:56.1084	**Velocity**	0.0	
		00:00:00			
	Calibrator	No			

Name	Position		Velocity		Group
ACT-CLJ0201.6-0503	Coordinate system	Equatorial	Convention	Optical	fall
	Equinox	J2000			
	Right Ascension	02:01:38.6644	Ref. frame	Barycentric	
		00:00:00			
	Declination	-5:03:20.507	Velocity	0.0	
		00:00:00			
	Calibrator	No			
ACT-CLJ0203.0-0042	Coordinate system	Equatorial	Convention	Optical	fall
	Equinox	J2000			
	Right Ascension	02:03:00.250317	Ref. frame	Barycentric	
		00:00:00			
	Declination	-00:42:25.9424	Velocity	0.0	
		00:00:00			
	Calibrator	No			
ACT-CLJ0203.2-0123	Coordinate system	Equatorial	Convention	Optical	fall
	Equinox	J2000			
	Right Ascension	02:03:15.7529	Ref. frame	Barycentric	
		00:00:00			
	Declination	-1:23:48.0291	Velocity	0.0	
		00:00:00			
	Calibrator	No			
ACT-CLJ0203.7+0216	Coordinate system	Equatorial	Convention	Optical	fall
	Equinox	J2000			
	Right Ascension	02:03:43.7951	Ref. frame	Barycentric	
		00:00:00			
	Declination	+02:16:04.09792	Velocity	0.0	
		00:00:00			
	Calibrator	No			
ACT-CLJ0203.9-0205	Coordinate system	Equatorial	Convention	Optical	fall
	Equinox	J2000			
	Right Ascension	02:03:57.0253	Ref. frame	Barycentric	
		00:00:00			
	Declination	-2:05:30.0	Velocity	0.0	
		00:00:00			
	Calibrator	No			
ACT-CLJ0204.5+0321	Coordinate system	Equatorial	Convention	Optical	fall
	Equinox	J2000			
	Right Ascension	02:04:31.9957	Ref. frame	Barycentric	
		00:00:00			
	Declination	+03:21:52.6144	Velocity	0.0	
		00:00:00			
	Calibrator	No			

Name	Position		Velocity		Group
ACT-CLJ0204.7-0116	**Coordinate system**	Equatorial	**Convention**	Optical	fall
	Equinox	J2000			
	Right Ascension	02:04:45.7503	**Ref. frame**	Barycentric	
		00:00:00			
	Declination	-1:16:56.3517	**Velocity**	0.0	
		00:00:00			
	Calibrator	No			
ACT-CLJ0204.8-0303	**Coordinate system**	Equatorial	**Convention**	Optical	fall
	Equinox	J2000			
	Right Ascension	02:04:50.2651	**Ref. frame**	Barycentric	
		00:00:00			
	Declination	-3:03:41.1831	**Velocity**	0.0	
		00:00:00			
	Calibrator	No			
ACT-CLJ0205.2-0439	**Coordinate system**	Equatorial	**Convention**	Optical	fall
	Equinox	J2000			
	Right Ascension	02:05:16.0926	**Ref. frame**	Barycentric	
		00:00:00			
	Declination	-4:39:11.2442	**Velocity**	0.0	
		00:00:00			
	Calibrator	No			
ACT-CLJ0205.9-0307	**Coordinate system**	Equatorial	**Convention**	Optical	fall
	Equinox	J2000			
	Right Ascension	02:05:59.2886	**Ref. frame**	Barycentric	
		00:00:00			
	Declination	-3:07:19.3178	**Velocity**	0.0	
		00:00:00			
	Calibrator	No			
ACT-CLJ0206.2-0114	**Coordinate system**	Equatorial	**Convention**	Optical	fall
	Equinox	J2000			
	Right Ascension	02:06:13.5751	**Ref. frame**	Barycentric	
		00:00:00			
	Declination	-1:14:34.075	**Velocity**	0.0	
		00:00:00			
	Calibrator	No			
ACT-CLJ0206.4-0118	**Coordinate system**	Equatorial	**Convention**	Optical	fall
	Equinox	J2000			
	Right Ascension	02:06:25.9909	**Ref. frame**	Barycentric	
		00:00:00			
	Declination	-1:18:30.1017	**Velocity**	0.0	
		00:00:00			
	Calibrator	No			

Name	Position		Velocity		Group
ACT-CLJ0206.9-0119	**Coordinate system**	Equatorial	**Convention**	Optical	fall
	Equinox	J2000			
	Right Ascension	02:06:57.0171	**Ref. frame**	Barycentric	
		00:00:00			
	Declination	-1:20:00.0	**Velocity**	0.0	
		00:00:00			
	Calibrator	No			
ACT-CLJ0207.2+0536	**Coordinate system**	Equatorial	**Convention**	Optical	fall
	Equinox	J2000			
	Right Ascension	02:07:12.1106	**Ref. frame**	Barycentric	
		00:00:00			
	Declination	+05:36:37.5638	**Velocity**	0.0	
		00:00:00			
	Calibrator	No			
ACT-CLJ0207.7+0020	**Coordinate system**	Equatorial	**Convention**	Optical	fall
	Equinox	J2000			
	Right Ascension	02:07:45.7478	**Ref. frame**	Barycentric	
		00:00:00			
	Declination	+00:20:57.0687	**Velocity**	0.0	
		00:00:00			
	Calibrator	No			
ACT-CLJ0208.2-0237	**Coordinate system**	Equatorial	**Convention**	Optical	fall
	Equinox	J2000			
	Right Ascension	02:08:15.587	**Ref. frame**	Barycentric	
		00:00:00			
	Declination	-2:37:18.0036	**Velocity**	0.0	
		00:00:00			
	Calibrator	No			
ACT-CLJ0208.3-0255	**Coordinate system**	Equatorial	**Convention**	Optical	fall
	Equinox	J2000			
	Right Ascension	02:08:20.6231	**Ref. frame**	Barycentric	
		00:00:00			
	Declination	-2:55:59.6276	**Velocity**	0.0	
		00:00:00			
	Calibrator	No			
ACT-CLJ0209.6+0222	**Coordinate system**	Equatorial	**Convention**	Optical	fall
	Equinox	J2000			
	Right Ascension	02:09:37.3266	**Ref. frame**	Barycentric	
		00:00:00			
	Declination	+02:22:40.3572	**Velocity**	0.0	
		00:00:00			
	Calibrator	No			

Name	Position		Velocity		Group
ACT-CLJ0209.9+0038	Coordinate system	Equatorial	Convention	Optical	fall
	Equinox	J2000			
	Right Ascension	02:10:00.0	Ref. frame	Barycentric	
		00:00:00			
	Declination	+00:38:14.8513	Velocity	0.0	
		00:00:00			
	Calibrator	No			
ACT-CLJ0210.0-0243	Coordinate system	Equatorial	Convention	Optical	fall
	Equinox	J2000			
	Right Ascension	02:10:01.0216	Ref. frame	Barycentric	
		00:00:00			
	Declination	-2:43:15.0489	Velocity	0.0	
		00:00:00			
	Calibrator	No			
ACT-CLJ0210.1+0254	Coordinate system	Equatorial	Convention	Optical	fall
	Equinox	J2000			
	Right Ascension	02:10:11.7265	Ref. frame	Barycentric	
		00:00:00			
	Declination	+02:54:25.9485	Velocity	0.0	
		00:00:00			
	Calibrator	No			
ACT-CLJ0211.1-0453	Coordinate system	Equatorial	Convention	Optical	fall
	Equinox	J2000			
	Right Ascension	02:11:12.0	Ref. frame	Barycentric	
		00:00:00			
	Declination	-4:53:44.5326	Velocity	0.0	
		00:00:00			
	Calibrator	No			
ACT-CLJ0211.2-0343	Coordinate system	Equatorial	Convention	Optical	fall
	Equinox	J2000			
	Right Ascension	02:11:14.7879	Ref. frame	Barycentric	
		00:00:00			
	Declination	-3:43:23.6529	Velocity	0.0	
		00:00:00			
	Calibrator	No			
ACT-CLJ0211.9-0146	Coordinate system	Equatorial	Convention	Optical	fall
	Equinox	J2000			
	Right Ascension	02:11:56.9173	Ref. frame	Barycentric	
		00:00:00			
	Declination	-1:46:10.0737	Velocity	0.0	
		00:00:00			
	Calibrator	No			

Name	Position		Velocity		Group
ACT-CLJ0212.5+0152	**Coordinate system**	Equatorial	**Convention**	Optical	fall
	Equinox	J2000			
	Right Ascension	02:12:30.6598	**Ref. frame**	Barycentric	
		00:00:00			
	Declination	+01:52:37.3158	**Velocity**	0.0	
		00:00:00			
	Calibrator	No			
ACT-CLJ0212.5-0037	**Coordinate system**	Equatorial	**Convention**	Optical	fall
	Equinox	J2000			
	Right Ascension	02:12:34.6632	**Ref. frame**	Barycentric	
		00:00:00			
	Declination	-00:37:33.5706	**Velocity**	0.0	
		00:00:00			
	Calibrator	No			
ACT-CLJ0214.7-0432	**Coordinate system**	Equatorial	**Convention**	Optical	fall
	Equinox	J2000			
	Right Ascension	02:14:42.9143	**Ref. frame**	Barycentric	
		00:00:00			
	Declination	-4:32:54.9115	**Velocity**	0.0	
		00:00:00			
	Calibrator	No			
ACT-CLJ0215.4+0030	**Coordinate system**	Equatorial	**Convention**	Optical	fall
	Equinox	J2000			
	Right Ascension	02:15:28.1838	**Ref. frame**	Barycentric	
		00:00:00			
	Declination	+00:30:41.4215	**Velocity**	0.0	
		00:00:00			
	Calibrator	No			
ACT-CLJ0215.4-0440	**Coordinate system**	Equatorial	**Convention**	Optical	fall
	Equinox	J2000			
	Right Ascension	02:15:28.0	**Ref. frame**	Barycentric	
		00:00:00			
	Declination	-4:40:15.1445	**Velocity**	0.0	
		00:00:00			
	Calibrator	No			
ACT-CLJ0215.6-0113	**Coordinate system**	Equatorial	**Convention**	Optical	fall
	Equinox	J2000			
	Right Ascension	02:15:36.5766	**Ref. frame**	Barycentric	
		00:00:00			
	Declination	-1:13:30.2439	**Velocity**	0.0	
		00:00:00			
	Calibrator	No			

Name	Position		Velocity		Group
ACT-CLJ0215.8-0041	Coordinate system	Equatorial	Convention	Optical	fall
	Equinox	J2000			
	Right Ascension	02:15:50.0063	Ref. frame	Barycentric	
		00:00:00			
	Declination	-00:41:59.8743	Velocity	0.0	
		00:00:00			
	Calibrator	No			
ACT-CLJ0217.7-0345	Coordinate system	Equatorial	Convention	Optical	fall
	Equinox	J2000			
	Right Ascension	02:17:43.7509	Ref. frame	Barycentric	
		00:00:00			
	Declination	-3:45:33.603	Velocity	0.0	
		00:00:00			
	Calibrator	No			
ACT-CLJ0217.8-0048	Coordinate system	Equatorial	Convention	Optical	fall
	Equinox	J2000			
	Right Ascension	02:17:48.7109	Ref. frame	Barycentric	
		00:00:00			
	Declination	-00:48:10.9724	Velocity	0.0	
		00:00:00			
	Calibrator	No			
ACT-CLJ0218.1-0214	Coordinate system	Equatorial	Convention	Optical	fall
	Equinox	J2000			
	Right Ascension	02:18:06.02808	Ref. frame	Barycentric	
		00:00:00			
	Declination	-2:14:21.1102	Velocity	0.0	
		00:00:00			
	Calibrator	No			
ACT-CLJ0218.2-0041	Coordinate system	Equatorial	Convention	Optical	fall
	Equinox	J2000			
	Right Ascension	02:18:16.2166	Ref. frame	Barycentric	
		00:00:00			
	Declination	-00:41:36.748	Velocity	0.0	
		00:00:00			
	Calibrator	No			
ACT-CLJ0218.5-0114	Coordinate system	Equatorial	Convention	Optical	fall
	Equinox	J2000			
	Right Ascension	02:18:34.2095	Ref. frame	Barycentric	
		00:00:00			
	Declination	-1:14:34.0888	Velocity	0.0	
		00:00:00			
	Calibrator	No			

Name	Position		Velocity		Group
ACT-CLJ0218.7-0014	Coordinate system	Equatorial	Convention	Optical	fall
	Equinox	J2000			
	Right Ascension	02:18:42.2134	Ref. frame	Barycentric	
		00:00:00			
	Declination	-00:14:37.9764	Velocity	0.0	
		00:00:00			
	Calibrator	No			
ACT-CLJ0219.0+0303	Coordinate system	Equatorial	Convention	Optical	fall
	Equinox	J2000			
	Right Ascension	02:19:02.6751	Ref. frame	Barycentric	
		00:00:00			
	Declination	+03:03:39.9509	Velocity	0.0	
		00:00:00			
	Calibrator	No			
ACT-CLJ0219.8+0022	Coordinate system	Equatorial	Convention	Optical	fall
	Equinox	J2000			
	Right Ascension	02:19:50.0975	Ref. frame	Barycentric	
		00:00:00			
	Declination	+00:22:26.4991	Velocity	0.0	
		00:00:00			
	Calibrator	No			
ACT-CLJ0219.9+0130	Coordinate system	Equatorial	Convention	Optical	fall
	Equinox	J2000			
	Right Ascension	02:19:54.6959	Ref. frame	Barycentric	
		00:00:00			
	Declination	+01:30:11.2079	Velocity	0.0	
		00:00:00			
	Calibrator	No			
ACT-CLJ0219.9+0246	Coordinate system	Equatorial	Convention	Optical	fall
	Equinox	J2000			
	Right Ascension	02:19:54.9673	Ref. frame	Barycentric	
		00:00:00			
	Declination	+02:46:59.955	Velocity	0.0	
		00:00:00			
	Calibrator	No			
ACT-CLJ0220.9-0332	Coordinate system	Equatorial	Convention	Optical	fall
	Equinox	J2000			
	Right Ascension	02:20:56.8771	Ref. frame	Barycentric	
		00:00:00			
	Declination	-3:32:52.3574	Velocity	0.0	
		00:00:00			
	Calibrator	No			

Name	Position		Velocity		Group
ACT-CLJ0221.6-0012	Coordinate system	Equatorial	Convention	Optical	fall
	Equinox	J2000			
	Right Ascension	02:21:36.5458	Ref. frame	Barycentric	
		00:00:00			
	Declination	-00:12:36.3921	Velocity	0.0	
		00:00:00			
	Calibrator	No			
ACT-CLJ0221.7-0346	Coordinate system	Equatorial	Convention	Optical	fall
	Equinox	J2000			
	Right Ascension	02:21:45.5181	Ref. frame	Barycentric	
		00:00:00			
	Declination	-3:46:22.2509	Velocity	0.0	
		00:00:00			
	Calibrator	No			
ACT-CLJ0221.9-0340	Coordinate system	Equatorial	Convention	Optical	fall
	Equinox	J2000			
	Right Ascension	02:21:55.5396	Ref. frame	Barycentric	
		00:00:00			
	Declination	-3:40:10.3875	Velocity	0.0	
		00:00:00			
	Calibrator	No			
ACT-CLJ0222.2+0520	Coordinate system	Equatorial	Convention	Optical	fall
	Equinox	J2000			
	Right Ascension	02:22:16.9953	Ref. frame	Barycentric	
		00:00:00			
	Declination	+05:20:14.9254	Velocity	0.0	
		00:00:00			
	Calibrator	No			
ACT-CLJ0223.1-0057	Coordinate system	Equatorial	Convention	Optical	fall
	Equinox	J2000			
	Right Ascension	02:23:09.41225	Ref. frame	Barycentric	
		00:00:00			
	Declination	-00:57:07.83138	Velocity	0.0	
		00:00:00			
	Calibrator	No			
ACT-CLJ0223.6+0020	Coordinate system	Equatorial	Convention	Optical	fall
	Equinox	J2000			
	Right Ascension	02:23:37.7531	Ref. frame	Barycentric	
		00:00:00			
	Declination	+00:20:56.0464	Velocity	0.0	
		00:00:00			
	Calibrator	No			

Name	Position		Velocity		Group
ACT-CLJ0224.5+0102	Coordinate system	Equatorial	Convention	Optical	fall
	Equinox	J2000			
	Right Ascension	02:24:30.0013	Ref. frame	Barycentric	
		00:00:00			
	Declination	+01:02:53.8298	Velocity	0.0	
		00:00:00			
	Calibrator	No			
ACT-CLJ0224.5-0002	Coordinate system	Equatorial	Convention	Optical	fall
	Equinox	J2000			
	Right Ascension	02:24:34.971	Ref. frame	Barycentric	
		00:00:00			
	Declination	-00:02:15.1573	Velocity	0.0	
		00:00:00			
	Calibrator	No			
ACT-CLJ0225.4-0355	Coordinate system	Equatorial	Convention	Optical	fall
	Equinox	J2000			
	Right Ascension	02:25:28.0314	Ref. frame	Barycentric	
		00:00:00			
	Declination	-3:56:00.0	Velocity	0.0	
		00:00:00			
	Calibrator	No			
ACT-CLJ0226.4+0426	Coordinate system	Equatorial	Convention	Optical	fall
	Equinox	J2000			
	Right Ascension	02:26:28.9505	Ref. frame	Barycentric	
		00:00:00			
	Declination	+04:26:44.9376	Velocity	0.0	
		00:00:00			
	Calibrator	No			
ACT-CLJ0227.6-0318	Coordinate system	Equatorial	Convention	Optical	fall
	Equinox	J2000			
	Right Ascension	02:27:38.7014	Ref. frame	Barycentric	
		00:00:00			
	Declination	-3:18:03.13213	Velocity	0.0	
		00:00:00			
	Calibrator	No			
ACT-CLJ0228.4+0030	Coordinate system	Equatorial	Convention	Optical	fall
	Equinox	J2000			
	Right Ascension	02:28:28.8786	Ref. frame	Barycentric	
		00:00:00			
	Declination	+00:30:36.7665	Velocity	0.0	
		00:00:00			
	Calibrator	No			

Name	Position		Velocity		Group
ACT-CLJ0229.6-0336	**Coordinate system**	Equatorial	**Convention**	Optical	fall
	Equinox	J2000			
	Right Ascension	02:29:38.5184	**Ref. frame**	Barycentric	
		00:00:00			
	Declination	-3:36:40.2661	**Velocity**	0.0	
		00:00:00			
	Calibrator	No			
ACT-CLJ0230.9+0248	**Coordinate system**	Equatorial	**Convention**	Optical	fall
	Equinox	J2000			
	Right Ascension	02:30:55.7114	**Ref. frame**	Barycentric	
		00:00:00			
	Declination	+02:48:13.6488	**Velocity**	0.0	
		00:00:00			
	Calibrator	No			
ACT-CLJ0231.7-0453	**Coordinate system**	Equatorial	**Convention**	Optical	fall
	Equinox	J2000			
	Right Ascension	02:31:44.6277	**Ref. frame**	Barycentric	
		00:00:00			
	Declination	-4:53:09.60126	**Velocity**	0.0	
		00:00:00			
	Calibrator	No			
ACT-CLJ0232.1+0230	**Coordinate system**	Equatorial	**Convention**	Optical	fall
	Equinox	J2000			
	Right Ascension	02:32:07.62449	**Ref. frame**	Barycentric	
		00:00:00			
	Declination	+02:30:48.2405	**Velocity**	0.0	
		00:00:00			
	Calibrator	No			
ACT-CLJ0232.7+0214	**Coordinate system**	Equatorial	**Convention**	Optical	fall
	Equinox	J2000			
	Right Ascension	02:32:47.0102	**Ref. frame**	Barycentric	
		00:00:00			
	Declination	+02:15:00.0	**Velocity**	0.0	
		00:00:00			
	Calibrator	No			
ACT-CLJ0232.7+0350	**Coordinate system**	Equatorial	**Convention**	Optical	fall
	Equinox	J2000			
	Right Ascension	02:32:46.2213	**Ref. frame**	Barycentric	
		00:00:00			
	Declination	+03:50:25.4251	**Velocity**	0.0	
		00:00:00			
	Calibrator	No			

Name	Position		Velocity		Group
ACT-CLJ0233.2+0211	Coordinate system	Equatorial	Convention	Optical	fall
	Equinox	J2000			
	Right Ascension	02:33:12.6548	Ref. frame	Barycentric	
		00:00:00			
	Declination	+02:11:50.1811	Velocity	0.0	
		00:00:00			
	Calibrator	No			
ACT-CLJ0233.2+0248	Coordinate system	Equatorial	Convention	Optical	fall
	Equinox	J2000			
	Right Ascension	02:33:13.3338	Ref. frame	Barycentric	
		00:00:00			
	Declination	+02:48:49.9974	Velocity	0.0	
		00:00:00			
	Calibrator	No			
ACT-CLJ0233.2+0448	Coordinate system	Equatorial	Convention	Optical	fall
	Equinox	J2000			
	Right Ascension	02:33:14.9906	Ref. frame	Barycentric	
		00:00:00			
	Declination	+04:48:30.0	Velocity	0.0	
		00:00:00			
	Calibrator	No			
ACT-CLJ0233.6-0530	Coordinate system	Equatorial	Convention	Optical	fall
	Equinox	J2000			
	Right Ascension	02:33:37.2565	Ref. frame	Barycentric	
		00:00:00			
	Declination	-5:30:29.2475	Velocity	0.0	
		00:00:00			
	Calibrator	No			
ACT-CLJ0233.7+0127	Coordinate system	Equatorial	Convention	Optical	fall
	Equinox	J2000			
	Right Ascension	02:33:43.4391	Ref. frame	Barycentric	
		00:00:00			
	Declination	+01:27:41.0631	Velocity	0.0	
		00:00:00			
	Calibrator	No			
ACT-CLJ0234.5-0107	Coordinate system	Equatorial	Convention	Optical	fall
	Equinox	J2000			
	Right Ascension	02:34:35.063	Ref. frame	Barycentric	
		00:00:00			
	Declination	-1:07:54.541	Velocity	0.0	
		00:00:00			
	Calibrator	No			

Name	Position		Velocity		Group
ACT-CLJ0234.6-0259	Coordinate system	Equatorial	Convention	Optical	fall
	Equinox	J2000			
	Right Ascension	02:34:38.4913	Ref. frame	Barycentric	
		00:00:00			
	Declination	-2:59:48.8555	Velocity	0.0	
		00:00:00			
	Calibrator	No			
ACT-CLJ0235.2-0323	Coordinate system	Equatorial	Convention	Optical	fall
	Equinox	J2000			
	Right Ascension	02:35:14.0169	Ref. frame	Barycentric	
		00:00:00			
	Declination	-3:23:15.018	Velocity	0.0	
		00:00:00			
	Calibrator	No			
ACT-CLJ0235.5-0005	Coordinate system	Equatorial	Convention	Optical	fall
	Equinox	J2000			
	Right Ascension	02:35:30.9931	Ref. frame	Barycentric	
		00:00:00			
	Declination	-00:06:00.0	Velocity	0.0	
		00:00:00			
	Calibrator	No			
ACT-CLJ0236.5+0106	Coordinate system	Equatorial	Convention	Optical	fall
	Equinox	J2000			
	Right Ascension	02:36:33.0023	Ref. frame	Barycentric	
		00:00:00			
	Declination	+01:06:44.7104	Velocity	0.0	
		00:00:00			
	Calibrator	No			
ACT-CLJ0236.7-0228	Coordinate system	Equatorial	Convention	Optical	fall
	Equinox	J2000			
	Right Ascension	02:36:42.9856	Ref. frame	Barycentric	
		00:00:00			
	Declination	-2:28:15.1509	Velocity	0.0	
		00:00:00			
	Calibrator	No			
ACT-CLJ0237.6-0423	Coordinate system	Equatorial	Convention	Optical	fall
	Equinox	J2000			
	Right Ascension	02:37:37.576	Ref. frame	Barycentric	
		00:00:00			
	Declination	-4:23:30.0828	Velocity	0.0	
		00:00:00			
	Calibrator	No			

Name	Position		Velocity		Group
ACT-CLJ0238.1+0306	**Coordinate system**	Equatorial	**Convention**	Optical	fall
	Equinox	J2000			
	Right Ascension	02:38:08.1337	**Ref. frame**	Barycentric	
		00:00:00			
	Declination	+03:06:11.6026	**Velocity**	0.0	
		00:00:00			
	Calibrator	No			
ACT-CLJ0239.3-0332	**Coordinate system**	Equatorial	**Convention**	Optical	fall
	Equinox	J2000			
	Right Ascension	02:39:21.9989	**Ref. frame**	Barycentric	
		00:00:00			
	Declination	-3:32:09.68614	**Velocity**	0.0	
		00:00:00			
	Calibrator	No			
ACT-CLJ0239.8-0134	**Coordinate system**	Equatorial	**Convention**	Optical	fall
	Equinox	J2000			
	Right Ascension	02:39:53.1323	**Ref. frame**	Barycentric	
		00:00:00			
	Declination	-1:34:44.4825	**Velocity**	0.0	
		00:00:00			
	Calibrator	No			
ACT-CLJ0240.0+0116	**Coordinate system**	Equatorial	**Convention**	Optical	fall
	Equinox	J2000			
	Right Ascension	02:40:03.4275	**Ref. frame**	Barycentric	
		00:00:00			
	Declination	+01:16:00.882782	**Velocity**	0.0	
		00:00:00			
	Calibrator	No			
ACT-CLJ0240.0+0303	**Coordinate system**	Equatorial	**Convention**	Optical	fall
	Equinox	J2000			
	Right Ascension	02:40:03.00504	**Ref. frame**	Barycentric	
		00:00:00			
	Declination	+03:03:15.1299	**Velocity**	0.0	
		00:00:00			
	Calibrator	No			
ACT-CLJ0241.2-0018	**Coordinate system**	Equatorial	**Convention**	Optical	fall
	Equinox	J2000			
	Right Ascension	02:41:16.3415	**Ref. frame**	Barycentric	
		00:00:00			
	Declination	-00:18:47.3351	**Velocity**	0.0	
		00:00:00			
	Calibrator	No			

Name	Position		Velocity		Group
ACT-CLJ0241.4-0433	Coordinate system	Equatorial	Convention	Optical	fall
	Equinox	J2000			
	Right Ascension	02:41:29.5772	Ref. frame	Barycentric	
		00:00:00			
	Declination	-4:33:12.1388	Velocity	0.0	
		00:00:00			
	Calibrator	No			
ACT-CLJ0242.2-0345	Coordinate system	Equatorial	Convention	Optical	fall
	Equinox	J2000			
	Right Ascension	02:42:16.4619	Ref. frame	Barycentric	
		00:00:00			
	Declination	-3:45:30.3104	Velocity	0.0	
		00:00:00			
	Calibrator	No			
ACT-CLJ0242.7-0226	Coordinate system	Equatorial	Convention	Optical	fall
	Equinox	J2000			
	Right Ascension	02:42:44.5105	Ref. frame	Barycentric	
		00:00:00			
	Declination	-2:26:24.554	Velocity	0.0	
		00:00:00			
	Calibrator	No			
ACT-CLJ0242.7-0450	Coordinate system	Equatorial	Convention	Optical	fall
	Equinox	J2000			
	Right Ascension	02:42:43.0344	Ref. frame	Barycentric	
		00:00:00			
	Declination	-4:50:45.0672	Velocity	0.0	
		00:00:00			
	Calibrator	No			
ACT-CLJ0242.9-0250	Coordinate system	Equatorial	Convention	Optical	fall
	Equinox	J2000			
	Right Ascension	02:42:57.0442	Ref. frame	Barycentric	
		00:00:00			
	Declination	-2:50:39.3399	Velocity	0.0	
		00:00:00			
	Calibrator	No			
ACT-CLJ0243.2+0256	Coordinate system	Equatorial	Convention	Optical	fall
	Equinox	J2000			
	Right Ascension	02:43:16.2522	Ref. frame	Barycentric	
		00:00:00			
	Declination	+02:56:34.1063	Velocity	0.0	
		00:00:00			
	Calibrator	No			

Name	Position		Velocity		Group
ACT-CLJ0245.2+0032	**Coordinate system**	Equatorial	**Convention**	Optical	fall
	Equinox	J2000			
	Right Ascension	02:45:14.4311	**Ref. frame**	Barycentric	
		00:00:00			
	Declination	+00:32:47.7734	**Velocity**	0.0	
		00:00:00			
	Calibrator	No			
ACT-CLJ0245.2+0407	**Coordinate system**	Equatorial	**Convention**	Optical	fall
	Equinox	J2000			
	Right Ascension	02:45:15.0173	**Ref. frame**	Barycentric	
		00:00:00			
	Declination	+04:07:14.1798	**Velocity**	0.0	
		00:00:00			
	Calibrator	No			
ACT-CLJ0245.2-0240	**Coordinate system**	Equatorial	**Convention**	Optical	fall
	Equinox	J2000			
	Right Ascension	02:45:13.5044	**Ref. frame**	Barycentric	
		00:00:00			
	Declination	-2:40:47.5473	**Velocity**	0.0	
		00:00:00			
	Calibrator	No			
ACT-CLJ0245.7-0028	**Coordinate system**	Equatorial	**Convention**	Optical	fall
	Equinox	J2000			
	Right Ascension	02:45:43.0077	**Ref. frame**	Barycentric	
		00:00:00			
	Declination	-00:28:29.8275	**Velocity**	0.0	
		00:00:00			
	Calibrator	No			
ACT-CLJ0245.8-0042	**Coordinate system**	Equatorial	**Convention**	Optical	fall
	Equinox	J2000			
	Right Ascension	02:45:50.8966	**Ref. frame**	Barycentric	
		00:00:00			
	Declination	-00:42:28.1123	**Velocity**	0.0	
		00:00:00			
	Calibrator	No			
ACT-CLJ0246.4+0429	**Coordinate system**	Equatorial	**Convention**	Optical	fall
	Equinox	J2000			
	Right Ascension	02:46:29.3501	**Ref. frame**	Barycentric	
		00:00:00			
	Declination	+04:29:40.1356	**Velocity**	0.0	
		00:00:00			
	Calibrator	No			

Name	Position		Velocity		Group
ACT-CLJ0247.3-0156	Coordinate system	Equatorial	Convention	Optical	fall
	Equinox	J2000			
	Right Ascension	02:47:23.4288	Ref. frame	Barycentric	
		00:00:00			
	Declination	-1:56:15.3679	Velocity	0.0	
		00:00:00			
	Calibrator	No			
ACT-CLJ0248.0-0331	Coordinate system	Equatorial	Convention	Optical	fall
	Equinox	J2000			
	Right Ascension	02:48:03.81459	Ref. frame	Barycentric	
		00:00:00			
	Declination	-3:31:55.9157	Velocity	0.0	
		00:00:00			
	Calibrator	No			
ACT-CLJ0248.2+0238	Coordinate system	Equatorial	Convention	Optical	fall
	Equinox	J2000			
	Right Ascension	02:48:13.2291	Ref. frame	Barycentric	
		00:00:00			
	Declination	+02:38:09.91129	Velocity	0.0	
		00:00:00			
	Calibrator	No			
ACT-CLJ0248.2-0216	Coordinate system	Equatorial	Convention	Optical	fall
	Equinox	J2000			
	Right Ascension	02:48:13.633	Ref. frame	Barycentric	
		00:00:00			
	Declination	-2:16:06.08148	Velocity	0.0	
		00:00:00			
	Calibrator	No			
ACT-CLJ0248.3+0122	Coordinate system	Equatorial	Convention	Optical	fall
	Equinox	J2000			
	Right Ascension	02:48:23.3507	Ref. frame	Barycentric	
		00:00:00			
	Declination	+01:22:20.3694	Velocity	0.0	
		00:00:00			
	Calibrator	No			
ACT-CLJ0248.3-0337	Coordinate system	Equatorial	Convention	Optical	fall
	Equinox	J2000			
	Right Ascension	02:48:21.3513	Ref. frame	Barycentric	
		00:00:00			
	Declination	-3:37:19.7006	Velocity	0.0	
		00:00:00			
	Calibrator	No			

Name	Position		Velocity		Group
ACT-CLJ0248.7-0019	Coordinate system	Equatorial	Convention	Optical	fall
	Equinox	J2000			
	Right Ascension	02:48:47.3692	Ref. frame	Barycentric	
		00:00:00			
	Declination	-00:19:32.7282	Velocity	0.0	
		00:00:00			
	Calibrator	No			
ACT-CLJ0248.9-0328	Coordinate system	Equatorial	Convention	Optical	fall
	Equinox	J2000			
	Right Ascension	02:48:57.6803	Ref. frame	Barycentric	
		00:00:00			
	Declination	-3:28:44.9646	Velocity	0.0	
		00:00:00			
	Calibrator	No			
ACT-CLJ0249.6+0210	Coordinate system	Equatorial	Convention	Optical	fall
	Equinox	J2000			
	Right Ascension	02:49:40.991	Ref. frame	Barycentric	
		00:00:00			
	Declination	+02:10:14.8045	Velocity	0.0	
		00:00:00			
	Calibrator	No			
ACT-CLJ0250.1+0008	Coordinate system	Equatorial	Convention	Optical	fall
	Equinox	J2000			
	Right Ascension	02:50:08.51355	Ref. frame	Barycentric	
		00:00:00			
	Declination	+00:08:15.7771	Velocity	0.0	
		00:00:00			
	Calibrator	No			
ACT-CLJ0253.5-0017	Coordinate system	Equatorial	Convention	Optical	fall
	Equinox	J2000			
	Right Ascension	02:53:33.5919	Ref. frame	Barycentric	
		00:00:00			
	Declination	-00:17:42.7469	Velocity	0.0	
		00:00:00			
	Calibrator	No			
ACT-CLJ0254.4-0538	Coordinate system	Equatorial	Convention	Optical	fall
	Equinox	J2000			
	Right Ascension	02:54:26.051	Ref. frame	Barycentric	
		00:00:00			
	Declination	-5:38:15.264	Velocity	0.0	
		00:00:00			
	Calibrator	No			

Name	Position		Velocity		Group
ACT-CLJ0256.5+0006	Coordinate system	Equatorial	Convention	Optical	fall
	Equinox	J2000			
	Right Ascension	02:56:31.9055	Ref. frame	Barycentric	
		00:00:00			
	Declination	+00:06:17.5711	Velocity	0.0	
		00:00:00			
	Calibrator	No			
ACT-CLJ0257.0-0300	Coordinate system	Equatorial	Convention	Optical	fall
	Equinox	J2000			
	Right Ascension	02:57:04.2681	Ref. frame	Barycentric	
		00:00:00			
	Declination	-3:00:56.0942	Velocity	0.0	
		00:00:00			
	Calibrator	No			
ACT-CLJ0258.4+0147	Coordinate system	Equatorial	Convention	Optical	fall
	Equinox	J2000			
	Right Ascension	02:58:28.0	Ref. frame	Barycentric	
		00:00:00			
	Declination	+01:47:44.5755	Velocity	0.0	
		00:00:00			
	Calibrator	No			
ACT-CLJ0259.4-0524	Coordinate system	Equatorial	Convention	Optical	fall
	Equinox	J2000			
	Right Ascension	02:59:27.0294	Ref. frame	Barycentric	
		00:00:00			
	Declination	-5:24:30.0	Velocity	0.0	
		00:00:00			
	Calibrator	No			
ACT-CLJ0259.8-0037	Coordinate system	Equatorial	Convention	Optical	fall
	Equinox	J2000			
	Right Ascension	02:59:52.6581	Ref. frame	Barycentric	
		00:00:00			
	Declination	-00:37:20.2577	Velocity	0.0	
		00:00:00			
	Calibrator	No			
ACT-CLJ0300.2+0125	Coordinate system	Equatorial	Convention	Optical	fall
	Equinox	J2000			
	Right Ascension	03:00:13.1303	Ref. frame	Barycentric	
		00:00:00			
	Declination	+01:25:07.42604	Velocity	0.0	
		00:00:00			
	Calibrator	No			

Name	Position		Velocity		Group
ACT-CLJ0301.5-0248	Coordinate system	Equatorial	Convention	Optical	fall
	Equinox	J2000			
	Right Ascension	03:01:32.3849	Ref. frame	Barycentric	
		00:00:00			
	Declination	-2:48:42.0193	Velocity	0.0	
		00:00:00			
	Calibrator	No			

Sessions:

Name	Session time (hours)	Repeat	Separation	LST minimum	LST maximum	Elevation minimum
fall	3.75	5	0 day	00:00:00	05:30:00	30

Session Constraints:

Name	Scheduling constraints	Comments
fall		

Session Source/Resource Pairs:

Session name	Source	Resource	Time
fall	ACT-CLJ0200.3+0019 ACT-CLJ0201.6-0211 ACT-CLJ0201.6-0503 ACT-CLJ0203.0-0042 ACT-CLJ0203.2-0123 ACT-CLJ0203.7+0216 ACT-CLJ0203.9-0205 ACT-CLJ0204.5+0321 ACT-CLJ0204.7-0116 ACT-CLJ0204.8-0303 ACT-CLJ0205.2-0439 ACT-CLJ0205.9-0307 ACT-CLJ0206.2-0114 ACT-CLJ0206.4-0118 ACT-CLJ0206.9-0119 ACT-CLJ0207.2+0536 ACT-CLJ0207.7+0020 ACT-CLJ0208.2-0237 ACT-CLJ0208.3-0255 ACT-CLJ0209.6+0222 ACT-CLJ0209.9+0038 ACT-CLJ0210.0-0243 ACT-CLJ0210.1+0254 ACT-CLJ0211.1-0453 ACT-CLJ0211.2-0343 ACT-CLJ0211.9-0146 ACT-CLJ0212.5+0152 ACT-CLJ0212.5-0037 ACT-CLJ0214.7-0432 ACT-CLJ0215.4+0030	M2 stuff (Shared Risk)	3.75 hour

Session name	Source	Resource	Time
	ACT-CLJ0215.4-0440		
	ACT-CLJ0215.6-0113		
	ACT-CLJ0215.8-0041		
	ACT-CLJ0217.7-0345		
	ACT-CLJ0217.8-0048		
	ACT-CLJ0218.1-0214		
	ACT-CLJ0218.2-0041		
	ACT-CLJ0218.5-0114		
	ACT-CLJ0218.7-0014		
	ACT-CLJ0219.0+0303		
	ACT-CLJ0219.8+0022		
	ACT-CLJ0219.9+0130		
	ACT-CLJ0219.9+0246		
	ACT-CLJ0220.9-0332		
	ACT-CLJ0221.6-0012		
	ACT-CLJ0221.7-0346		
	ACT-CLJ0221.9-0340		
	ACT-CLJ0222.2+0520		
	ACT-CLJ0223.1-0057		
	ACT-CLJ0223.6+0020		
	ACT-CLJ0224.5+0102		
	ACT-CLJ0224.5-0002		
	ACT-CLJ0225.4-0355		
	ACT-CLJ0226.4+0426		
	ACT-CLJ0227.6-0318		
	ACT-CLJ0228.4+0030		
	ACT-CLJ0229.6-0336		
	ACT-CLJ0230.9+0248		
	ACT-CLJ0231.7-0453		
	ACT-CLJ0232.1+0230		
	ACT-CLJ0232.7+0214		
	ACT-CLJ0232.7+0350		
	ACT-CLJ0233.2+0211		
	ACT-CLJ0233.2+0248		
	ACT-CLJ0233.2+0448		
	ACT-CLJ0233.6-0530		
	ACT-CLJ0233.7+0127		
	ACT-CLJ0234.5-0107		
	ACT-CLJ0234.6-0259		
	ACT-CLJ0235.2-0323		
	ACT-CLJ0235.5-0005		
	ACT-CLJ0236.5+0106		
	ACT-CLJ0236.7-0228		
	ACT-CLJ0237.6-0423		
	ACT-CLJ0238.1+0306		
	ACT-CLJ0239.3-0332		
	ACT-CLJ0239.8-0134		
	ACT-CLJ0240.0+0116		
	ACT-CLJ0240.0+0303		
	ACT-CLJ0241.2-0018		
	ACT-CLJ0241.4-0433		
	ACT-CLJ0242.2-0345		
	ACT-CLJ0242.7-0226		
	ACT-CLJ0242.7-0450		
	ACT-CLJ0242.9-0250		

Session name	Source	Resource	Time
	ACT-CLJ0243.2+0256 ACT-CLJ0245.2+0032 ACT-CLJ0245.2+0407 ACT-CLJ0245.2-0240 ACT-CLJ0245.7-0028 ACT-CLJ0245.8-0042 ACT-CLJ0246.4+0429 ACT-CLJ0247.3-0156 ACT-CLJ0248.0-0331 ACT-CLJ0248.2+0238 ACT-CLJ0248.2-0216 ACT-CLJ0248.3+0122 ACT-CLJ0248.3-0337 ACT-CLJ0248.7-0019 ACT-CLJ0248.9-0328 ACT-CLJ0249.6+0210 ACT-CLJ0250.1+0008 ACT-CLJ0253.5-0017 ACT-CLJ0254.4-0538 ACT-CLJ0256.5+0006 ACT-CLJ0257.0-0300 ACT-CLJ0258.4+0147 ACT-CLJ0259.4-0524 ACT-CLJ0259.8-0037 ACT-CLJ0300.2+0125 ACT-CLJ0301.5-0248		

Plan of dissertation: no

Technical Justification:

Dates:

n/a

Observing time:

standard mustang-2 configurations, hardware

Mapping:

we use the standard information at
www.gb.nrao.edu/mustang
which says we can map in one hour (integration time) a R~3' (D~6') area - which is what we're aiming for here - to 56 uJy. we want about 200 uJy/bm RMS, which takes 4.7min (integration time), rounded up to 5min at the level of accuracy of our sensitivity numbers.
Double that for total telescope time with calibration, slewing, all overheads.

This approach, including the new, wider shallower mapping, has been demonstrated successfully in GBT21B_298

RFI considerations:

n/a still hopefully...

Overhead:

standard factor of 2

Joint considerations:

n/a

Novel considerations:

n/a

Pulsar considerations:

n/a

LST Range Justification:

I had multi-source groups, and the min/max LST calculation didn't seem to work. so I did it by hand.

Measuring the 3mm Source Population in an SZ-selected Galaxy Cluster Sample

Objective: To precisely quantify the incidence and characteristics of discrete sources— such as active galactic nuclei and star forming galaxies— on sight-lines near galaxy clusters selected by current and future Sunyaev-Zel'dovich Effect (SZE) surveys. *This is a resubmission of our partially successful program 21B-298 which was awarded* $50.75h$*,* $30.25h$ *was scheduled on the GBT before it expired.*

Scientific Motivation: Galaxy clusters are the most massive virialized objects known, and their study has long provided crucial information about cosmology, including the first indications of dark matter (Zwicky 1937), early indications of a low total matter density Ω_m (Bahcall & Cen 1992), and distance-ladder independent estimates of the Hubble constant (Reese et al. 2002, Udomprasert et al. 2004). The important role of clusters in informing our understanding of cosmology has continued in the modern era of precision cosmology. The Dark Energy Survey (DES), for instance, has surveyed a $5,000\,\mathrm{deg}^2$ region of the Southern sky and expects to find over 200,000 galaxy clusters (by photometric "Red Sequence" selection) as well as measuring weak lensing from clusters and larger scale cosmic structures (Dark Energy Survey Collaboration, 2016). Millimeter-wave surveys using the Sunyaev-Zel'dovich Effect (SZE) are a crucial, recent development since they provide an approximately mass-limited and nearly redshift-independent[1] sample of galaxy clusters. These characteristics have driven large-scale SZE surveys, most notably those conducted by the Atacama Cosmology Telescopes (ACT: Hilton et al. 2020) and the South Pole Telescope (SPT: Bleem et al. 2020). Next-generation SZE surveys will also be carried out by the Simons Observatory (SO: Ade et al. 2019) and CMB S4 (Abazajian et al. 2016). To realize the sub-percent cosmological constraints that these surveys aim to provide it is essential to quantitatively understand relevant systematic errors and biases. With this proposal, we aim to directly address one potential source of bias in SZE-selected cluster samples: extragalactic foreground and background sources. We specifically focus on the ACT DR5 cluster catalog (Hilton et al. 2020), which has significant sky coverage going up to $\delta = +20^\circ$, and is directly observable by the GBT.

For SZE surveys, two leading systematic errors are the scatter in the mass-SZE relationship and contamination by extragalactic foreground, background, and cluster-centric sources. The contaminating sources broadly fall into two, non-mutually exclusive categories: active galactic nuclei or AGN— traditional "radio sources", with flux densities typically following a synchrotron ($S_\nu \sim \nu^{-0.7}$) spectrum; and dusty star forming galaxies (SFGs), which typically evince modified black body spectra ($S_\nu \sim \nu^3$ at cm and mm wavelengths). ACT mitigates source contamination by searching for bright, positive, compact sources in its 150 GHz band ($S_{150} > 10\,\mathrm{mJy}$) and masking the corresponding sky area. The ACT DR5 cluster search footprint has an area of $13,484\,\mathrm{deg}^2$ after Galactic latitude and dust cuts; $\sim 11,000$ discrete sources are found in this area, resulting in 2% of the survey area being masked. While the fraction of data so lost may seem small, there are two significant limitations to this technique. First, at the ACT resolution of $1'.4$ - $2'.2$, the (positive) discrete source signals and the SZE decrement can be degenerate, with the result that only the brightest discrete sources can be reliably detected. Fainter sources will evade the detection threshold and partially (or completely) "fill in" the SZE decrement at 98 and 150 GHz, the most sensitive SZ bands for current and next generation ACT. Second, the relationship between galaxy clusters and these discrete sources (and therefore the survey mask)— and the redshift and cluster mass dependence of that relationship— is a complex topic the details of which are still under active investigation. Broadly speaking, the co-moving spatial density of AGN (at fixed luminosity) is well understood to have been at least an order of magnitude higher at

[1] SZE surveys are usually incomplete at low redshifts where the cluster signal becomes much larger than the instrument beam; although for very low-resolution instruments like *Planck* beam dilution will generate incompleteness at high redshift.

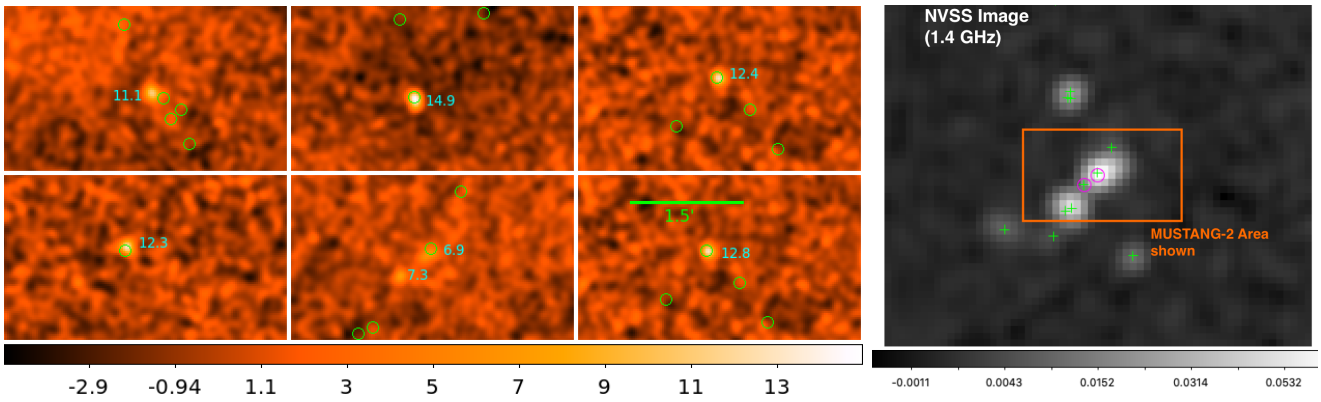

Figure 1: **Left:** Six MUSTANG-2 signal-to-noise maps of ACT cluster fields from our program GBT21B-298. Sources are identified by a 10″ Gaussian matched filter which well approximates the GBT 3mm beam; the peak SNR for each source is labeled in *cyan*. *Green circles* indicate the locations of NVSS sources. Note that at this depth the cluster SZE is not expected to be visible. **Right:** The NVSS 1.4 GHz image (in Jy/NVSS beam) of the field in the lower center of the left 6 panels. The 3mm map clearly detects one lobe of this classic, double-lobed radio jet, but not the other; the 3mm map also detects a core component, missed in NVSS but detected by FIRST. Here *magenta circles* show the locations of detected 3mm sources, while *green crosses* show the locations of FIRST 1.4 GHz sources. The diversity of spectral characteristics we see— combined with the density of low frequency radio sources— illustrate the need for sensitive 3mm imaging to identify and characterize the contaminating population of sources.

high redshift ($z > 0.8$) than in the local universe (e.g., Dunlop & Peacock 1990, De Zotti et al. 2010, Mo et al. 2020). Similar results obtain for star forming galaxies although, perhaps surprisingly, AGN dominate the discrete source counts seen in 150 GHz blind surveys at the detection limit achieved by ACT (Gralla et al. 2020). In the local universe ($z < 0.25$), luminous AGN are more rare in clusters than in the field (Kauffman et al. 2004), but lower luminosity AGN are probably not (Martini et al. 2002). At $z > 1$ however, the fraction of clusters hosting AGN is $\sim 30\times$ higher and comparable to the field population at those redshifts (Martini et al. 2014), indicating rapid evolution in the cluster AGN fraction over the redshift range where most ACT and SPT clusters are detected (median $z \sim 0.5$). Interestingly, a study of ~ 600 optically selected (red sequence) galaxy clusters found little evidence for excess 1.4 GHz radio source activity compared to the field in a more limited range $0.35 < z < 0.95$, although there were indications that non-BCG cluster members were more likely to be radio-active at higher z (Gralla et al. 2011). It is essential to understand these evolutionary effects and selection biases quantitatively in order to fully achieve the science goals of current and near future SZE surveys such as Advanced ACT, Simons Observatory, and CMB S4.

Our own SZE observations with MUSTANG-2 on the GBT over the past decade allow us to estimate the magnitude of source contamination for SZE-selected clusters and suggest that this issue is more significant than previously appreciated (Dicker et al. 2021). We have been using MUSTANG-2 and its predecessor (MUSTANG) on the GBT to conduct targeted, high-resolution (10″) imaging of the SZE on several dozen clusters over in a variety of programs (e.g. Korngut et al. 2011, Mroczkowski et al. 2012, Romero et al. 2017, Dicker et al. 2020, Okabe et al. 2021). To assess the impact of discrete sources on SZE-derived masses, we assembled maps of 30 galaxy clusters from these programs and searched them for discrete sources. Fully 60% of clusters show detectable discrete sources, and 20% of clusters have an integrated, 3mm discrete source flux density of 1 mJy or greater. Allowing for the

ACT DR5 source-masking strategy, we find on average 0.8 mJy of 3mm flux density from residual (un-identified by ACT) discrete sources. Because of shot noise there is a positive tail to the distribution: the standard deviation of the residual flux is 1.2 mJy. Due to the small sample size— 30 clusters, with the residual flux dominated by fewer than 10 individual sources— the statistical uncertainty in these estimates is $\sim 30\%$. The systematic uncertainty due to the heterogeneously selected underlying cluster sample is also of concern, and is far more difficult to quantify. Low-frequency radio surveys such as NVSS offer some potentially useful information, but large scatter in the spectral indices is problematic: Dicker et al. find 3mm-detected sources have typical spectral indices $\alpha_{1.4-90} = -0.48$ with a standard deviation of 0.30. This prohibits, for instance, directly identifying the problematic sources from NVSS and masking them in the ACT data.

Dicker et al. carried out simulations to assess the impact of un-masked point sources on the ACT cluster catalog which take into account the dual-frequency (90 and 150 GHz) matched filter used to find the clusters (Hilton et al. 2020). We find that 9% of clusters are contaminated by 10% or more by un-masked discrete sources; these sources contribute an overall scatter of 6% to the ACT SZ-derived mass estimates. We further estimate up to 5% incompleteness in the ACT DR5 cluster catalog due to residual source contamination. *These results show that residual discrete sources are an important systematic which need to be better understood and, if possible, controlled.* Our ability to do so from existing data is limited by both small number statistics, and by the heterogeneous sample on which the analysis is based. This proposal aims to address both of these limitations. We are also submitting a companion 22B proposal (PI: Simon Dicker) to study the important, related question of SZE cluster survey completeness in comparison with x-ray cluster catalogs.

Sample Selection, Progress & Proposed Observations: All clusters have been selected from the ACT SZE cluster catalog (Hilton et al. 2020), all of which have been optically confirmed. No mass limit will be imposed, allowing us to probe the properties of the sample as a whole. We further impose the following criteria. First, we select targets with Right Ascensions favorable for night-time (high frequency) observations in the Northern Fall, Winter or Spring. Based on past experience with GBT 3mm observations we have chosen the range $2h$ to $16h$. Second, in order to facilitate identification and classification of sources, we restrict our sample to those which lie within the footprints of the Dark Energy Survey (DES: Dark Energy Survey Collaboration, 2016), the Hyper Suprime Cam Survey (HSC: Aihara et al. 2018), or the Kilo-degree Survey (KiDS: Wright et al. 2019). All targets are also within the footprint of the NRAO VLA Sky Survey (NVSS: Condon et al. 1998) and the new VLA Sky Survey (VLASS: Lacy et al. 2020). Finally, to facilitate efficient GBT 3mm observations— also guided by the lower declination limits of KiDS and HSC— we select targets with $\delta > -6°$. **These selection criteria result in a sample of 300 galaxy clusters** (summarized in Table 1). During semester 21B 30 hours of our survey (of 50 hours awarded) were scheduled on the GBT. After setting aside observations compromised by poor weather— most of our one early fall observing session— we have imaged 129 of these 300 clusters to noise levels below our 200 μJy/bm goal; the average image noise is actually $\sim 150\,\mu$Jy/bm (discussed further below). Some first look images from our recent observations are in Figure 1. A preliminary processing of 92 clusters indicates that $\sim 10\%$ of clusters have at least one source above a very conservative $S_{3mm} = 1$ mJy/bm limit. This is in line with expectations from our earlier work (Dicker et al. 2021). Interestingly we find that only half of the 3mm sources we detect have NVSS counterparts. *We are requesting in this proposal the time to finish the 111 early Fall targets in our survey, which will bring our survey to 80% completion.* We will request the remaining (springtime) targets at the August 1 deadline.

We aim for a 5σ detection limit of $S_{3mm} = 1.0$ mJy. This will detect any source which, individually, contaminates the 98 GHz ACT SZE decrement by 2% for a median cluster (4% at the survey limit).

Field	RA Range	Dec. Range	N_{cl}	Complementary datasets
Fall	$2h - 3h$	$-6° - +6°$	111	DES, HSC, XMM-LSS
Winter	$8.5h - 11h$	$-3° - +4°$	94	KiDS-N-W2, HSC
Late Winter/Spring	$11h - 16h$	$-4° - +5°$	95	KiDS-N

Table 1: Fields selected for our cluster survey, grouped by time of year with optimal northern nighttime visibility. RA and Dec. ranges are approximate. Two of our targets have potentially helpful ALMA 3mm mosaic images available, though the fields of view are smaller than those we propose ($< 3'$); a further three clusters also have ALMA 1mm mosaics, also with relatively small fields of view.

This limit corresponds to 5 minutes of integration time on sky using our standard "daisy petal" scan pattern. Much shorter integration times are not efficient due to slewing overheads. We have demonstrated that 5 minutes of observations using our proposed scan strategy will result in well-sampled sky coverage within a $D \sim 6'$ region. We also find, as expected, that more aggressive filtering in the reduction pipeline reduces the noise by about 25% at the expense of filtering out larger scale spatial structures. Since our program aims to characterize sources that are generally compact at this resolution ($9''$), we expect to achieve a 5σ detection limit close to 0.7 mJy. **Including overheads our total time request is** 18.75 **hours of excellent nighttime high frequency GBT time in the early fall**. This will bring our sample to 80% completion. The remaining 20% will require ~ 10 hours of springtime observing.

Analysis Plan & Expected Outcomes: The imaging and source search strategies will be similar to those described in Dicker et al. (2021). The result will be an unprecedentedly accurate measurement of the mean discrete-source contamination in SZE-selected galaxy clusters that is accurate to 5%, as well as (crucially) a measurement of the scatter in the source contamination level. The measurement will be made on a representative sample and so will be directly applicable to the interpretation of other SZE-selected samples in the future, such as CMB S4 and SO. We will also explore the extent to which existing surveys— particularly NVSS and VLASS, supplemented by WISE and deep optical data— can accurately predict the residual source contamination and potentially improve source-masking techniques. For example, using our 3mm maps it may be possible to identify the most problematic sources from NVSS and VLASS flux densities and morphologies. This information would be directly usable to improve the science yield from SZ search and analysis pipelines. Unlike the observations that are the basis of most of what we currently know about radio source populations, our survey will have been carried out directly at a frequency of key interest to the SZE surveys, minimizing systematic uncertainties associated with extrapolation in frequency.

When our survey paper is published we will make all maps and source catalogs available in a public, digital data repository such as Harvard's Dataverse or Zenodo.

References:

Abazajian et al. 2016, arXiv:1610.02743 • Ade et al. 2019, JCAP 2, 56 • Aihara et al. 2018, PASJ 70,4 • Bahcall & Cen 1992, ApJ 398, 81 • Bleem et al. 2020, ApJS 247, 28 • Condon et al. 1998, AJ 115, 1693 • Dark Energy Collaboration 2016, MNRAS 460, 1270 • De Zotti et al. 2010, A&AR 18,1 • Dicker et al. 2020, ApJ 902, 144 • Dicker et al. 2021, MNRAS 508, 2600 • Dunlop & Peacock 1990, MNRAS 247, 19 • Gralla et al. 2011, 734, 104 • Gralla et al. 2020, ApJ 893, 104 • Hilton et al. 2020, ApJ in press (arXiv:2009.11043) • Kauffmann et al. 2004, MNRAS 353, 713 • Korngut et al. 2011, ApJ 734, 10 • Lacy et al. 2020, PASP 132, 1009 • Martini et al. 2002, ApJ 576, 109 • Martini et al. 2013, ApJ 768, 1 • Mo et al. 2020, ApJ 901, 131 • Mroczkowski et al. 2012, ApJ 761, 47 • Okabe et al. 2021, MNRAS 501, 1701 • Reese et al. 2002, ApJ 581, 53 • Romero et al. 2017, ApJ 838, 86 • Udomprasert et al. 2004, ApJ 615, 63 • Wright et al. 2010, AJ 140, 1868 • Wright et al. 2019, A&A 632, 34 • Zwicky 1937, ApJ 86, 217